HHS Public Access

Author manuscript

J Immunol. Author manuscript; available in PMC 2021 February 01.

Published in final edited form as:

J Immunol. 2020 August 01; 205(3): 567–572. doi:10.4049/jimmunol.2000412.

Cutting Edge: Inhibition of the interaction of NK inhibitory receptors with MHC class I augments anti-viral and anti-tumor immunity

Abir K. Panda[1], **Arunakumar Gangaplara**[2], **Maja Buszko**[1], **Kannan Natarajan**[3], **Lisa F. Boyd**[3], **Suveena Sharma**[1], **David H. Margulies**[3], **Ethan M. Shevach**[1]

[1]Cellular Immunology Section, Laboratory of Immune System Biology, National Institute of Allergy and Infectious Diseases, Bethesda, MD, USA

[2]Laboratory of Early Sickle Mortality Prevention, National Heart, Lung and Blood Institute, National Institutes of Health, Bethesda, MD, USA

[3]Molecular Biology Section, Laboratory of Immune System Biology, National Institute of Allergy and Infectious Diseases, Bethesda, MD, USA

Abstract

NK cells recognize MHC-I antigens via stochastically expressed MHC-I-specific inhibitory receptors that prevent NK cell activation via cytoplasmic immunoreceptor tyrosine based inhibitory motifs. We have identified a pan-anti-MHC-I mAb which blocks NK cell inhibitory receptor binding at a site distinct from the TCR binding site. Treatment of unmanipulated mice with this mAb disrupted immune homeostasis, markedly activated NK and memory phenotype T cells, enhanced immune responses against transplanted tumors and augmented responses to acute and chronic viral infection. mAbs of this type represent novel check point inhibitors in tumor immunity, potent tools for the eradication of chronic infection, and may function as adjuvants for the augmentation of the immune response to weak vaccines.

Introduction

NK cells are a component of the innate immune system and play critical roles in the control of viral and tumor immunity as well as in the promotion of T cell-mediated adaptive immunity (1). NK cells recognize MHC-I antigens via stochastically expressed MHC-I-specific inhibitory receptors, members of the Ly49 family in mice and Killer Immunoglobulin-like Receptor (KIR) family in humans, that prevent NK cell activation via cytoplasmic immunoreceptor tyrosine based inhibitory motifs (2). Loss of MHC-I expression on tumors, antigen presenting cells, or targets (“missing self”) abrogates inhibitory signals resulting in NK activation (3, 4). Structural studies and competition experiments have shown that the binding site on MHC-I for Ly49 inhibitory receptors is

Address correspondence and reprint requests to Dr. Ethan Shevach, Laboratory of Immune System Biology, NIAID, NIH, Blg. 10, RM 11N315, Bethesda, MD 20892. eshevach@niaid.nih.gov.

Disclosures

The authors have no financial conflicts of interest.

distinct from that for TCRs (5, 6). We have identified a pan-anti-MHC-I mAb which blocks NK cell inhibitory receptor binding at a site distinct from the TCR binding site. Treatment of unmanipulated mice with this mAb disrupted immune homeostasis characterized by marked proliferation and activation of NK cells and $CD8^+$ and $CD4^+$ memory phenotype (MP) T cells. Activated NK cells secreted high amounts of IFN-γ that activated APC to produce elevated levels of IL-15 which further activated NK cells and drove MP T cell proliferation. The global disruption of NK cell/MHC-I interactions significantly enhanced immune responses against transplanted tumors and augmented responses to acute and chronic viral infection.

Materials and Methods

Mice

Female C57BL/6 and BALB/c mice were purchased from Charles River Laboratories. OT-I mice were purchased from the Jackson Laboratory. All mice were 8–12 weeks old and and all animal protocols used in this study were approved by National Institutes of Allergy and Infectious Diseases Animal Care and Use committee.

In vivo antibody treatment

Rat-IgG2a (250μg/dose, i.p., Clone 2A3, BioXcell) and Anti-MHC-I (500μg/dose, Clone M1/42, BioXcell), anti-H2-K^b (500μg/dose, Clone AF6–88.5, BioXcell), and anti-H2-D^b (Clone 28–14-8, made in house (7) were administrated every other day for 6 d. Anti-CD122 (350μg/dose, Clone TMβ1, BioXcell) or anti-IFNγ (500μg/dose, Clone XMG22.1, BioXcell) were given every other day for 6 d.

Lymphocyte Isolation

Lymphocytes from spleen were washed and suspended in sterile complete RPMI medium. Liver lymphocytes were isolated by Percoll mediated centrifugation.

NK cell and CD8 T cell depletion

For NK cell or CD8 T cell depletion, 400ug/dose anti-NK1.1 (clone: PK136, Bioxcell) or anti-CD8 (Clone: 2.43, Bioxcell) were treated intra-peritoneally (i.p) on two day before followed by anti-MHCI co-treatment every 3 days starting from day 0 and ending on day 15.

RNA purification and Quantitative Real time PCR

Total RNA was isolated from FACS sorted cells and transcribed into cDNA. Quantitative PCR was performed using predesigned primer and probe sets.

Flowcytometry

Fluorochrome conjugated antibodies were purchased from BD Biosciences, Biolegend, R&D Systems, and ThermoFisher Scientific. Staining with biotinylated recombinant Ly49A or Ly49C was performed as described previously (8). LCMV tetramer staining was performed as previously described (9). Melanoma-specific cells were detected with H2-D^b GP100 and H2-D^b Trp1 tetramers (NIH Tetramer Core Facility). All flow cytometric

experiments (data acquisition) were performed using BD Fortessa II flow cytometer and FACS-Diva software (BD Biosciences) and analyzed by Flowjo v.10.3 software (TreeStar).

Lymphocytic choriomeningitis virus (LCMV) infection

Acute and chronic LCMV infection were performed as previously described (9).

Tumor models

Female C57BL/6 mice were injected with MC38 cells (2×10^5) or B16F10 (1.25×10^5) cells s.c. in the right flank region. Tumor volumes (Length x Breadth x Height) were monitored by digital calipers.

Cell trace violet proliferation assay

Splenocytes from OT-I mice were stained with cell trace violet (CTV), pre-incubated with purified mAbs (50μg/well) for 1 hour, washed, and then cultured with $OVA_{257–264}$ (2.5μg/ml) for 48 h. CTV dilution was assayed by flow cytometry.

Statistical analysis

P values of mouse datasets were determined by paired or unpaired two-tailed Student's t-test with a 95% confidence interval. Where appropriate, Mann–Whitney U-test, Wilcoxon matched-pairs test or two-way ANOVA followed by Bonferroni post-tests were performed. All statistical tests were performed with Graph Pad Prism v.6 software. P values of less than 0.05 were considered to be significant.

Results and Discussion

As NK inhibitory murine Ly49 receptors bind to MHC-I by via contacts beneath the floor of the peptide binding groove as well residues of the β_2-microglobulin (β_2m) light chain (6, 10, 11), we reasoned that an antibody to this site would disrupt Ly49/MHC-I interactions resulting in a loss of immune homeostasis. Additionally, such an antibody would fail to inhibit the binding of alloantibodies primarily directed to polymorphic regions of the MHC-I molecule, but would be blocked by antibodies to β_2m. In competitive binding studies, one rat anti-mouse pan-anti-MHC-I antibody (M1/42) (12) met these criteria with respect to some, but not all alloantibodies. The binding of M1/42 to H-2^b MHC-I was completely blocked by an anti-β_2m mAb and *vice versa*, while neither of these mAbs had any effect on the binding of a mixture of allospecific-anti-MHC-I mAb (Fig. 1A). The binding of recombinant Ly49A to the MHC-I molecule, H2-D^d, was blocked by M1/42, and an anti-H2-K^d/D^d mAb (34–1-2S), but not by the anti-α3 domain specific 34–2-12 mAb (Fig. 1B). Similarly, Ly49C binding to either BALB/c (H-2^d) (Fig. 1B) or C57BL/6 (H-2^b) (Fig. 1C) splenocytes was blocked by M1/42. The anti-β_2m mAb also blocked Ly49C/H-2^b interaction (Fig. 1C). M1/42 had no effect on the antigen-specific proliferative response of $CD8^+$ T cells from OT-I transgenic mice which express a TCR specific for the SIINFEKL peptide derived from ovalbumin in association with H2-K^b (Fig. 1D), indicating that M1/42 recognizes a region distinct from the peptide/MHC TCR combining site.

To determine whether blocking of the binding of NK cell inhibitory receptors (NKIR) to MHC-I would have any functional effects on NK cells, we administered M1/42 or mAbs to polymorphic MHC-I determinants or anti-β_2m to unmanipulated mice for six d. Surprisingly, M1/42 dramatically altered immune homeostasis, as treatment with this mAb enhanced the proliferation of splenic NK cells, but did not lead to an increase in their absolute numbers, indicating that increased proliferation was balanced by cell death (Fig 1E). $CD4^+$ effector memory (EM, $CD4^+Foxp3^-CD44^+CD62L^-$) T cells proliferated and expanded following M1/42 treatment (Fig. 1F). Additionally, $CD8^+$ central memory (CM, $CD8^+CD44^+CD62L^+$) and $CD8^+$ effector memory (EM, $CD8^+CD44^+CD62L^-$) T cells proliferated and expanded (Fig. 1G, H) with dramatic enhancement of the frequency and absolute number of the $CD8^+$ EM population. Anti-β_2m had minimal effect on NK cell proliferation and no effect on $CD4^+$ and $CD8^+$ T cells (data not shown).

The *in vivo* proliferation of NK cells was dependent on the presence of IFN-γ (Fig. 2A), while the proliferation of MP T cells was dependent on both NK cells and IFN-γ (Fig. 2B–D). The enhancement of proliferation following M1/42 treatment was accompanied by a marked increase of cytokine (IFN-γ, TNF-α) and perforin/granzyme production by NK cells, as well as MP $CD4^+$ and $CD8^+$ populations (Fig. 2E–G). Treatment with mouse mAbs recognizing alloantigenic MHC-I determinants modestly enhanced NK cell, MP $CD4^+$ and $CD8^+$ T cell proliferation, and slightly enhanced their absolute numbers (Supplemental Fig. 1A–F), but had no effect on cytokine or cytotoxic granule production (Supplemental Fig.1G, H). Neither M1/42 nor the alloantibodies had any effects on number or frequency of T regulatory cells (Data not shown).

While a high percentage of NK cells (~80%) were induced to proliferate by M1/42 treatment, it remained possible that the proliferating population on day 8 represented a selected subpopulation of NK cells expressing a unique pattern of NKIR and/or NK cell activating receptors. M1/42 enhanced the proliferation of all Ly49-expressing (both activating and inhibitory) NK cell subpopulations equally as measured by Ki-67 staining (Supplemental Fig. 2). When analyzed on d 8, the percentage of cells expressing Ly49 activation receptors (Ly49D and Ly49H) was downregulated, whereas the subpopulation expressing inhibitory receptors (Ly49A, Ly49C, Ly49G2, and Ly49I) remained unchanged except for Ly49F which increased (Supplemental Fig. 2B). NK cell activation receptors that recognize non-MHC-I ligands (NKG2D and NKp46) were significantly downregulated, but the inhibitory NKG2A receptor remained unaltered (Supplemental Fig. 2C). These results are more compatible with a pan-NK cell enhanced proliferation rather than any specific subpopulation. The expression of the KLRG1 antigen on NK cells is postulated to prevent NK cell activation by inhibiting IFNγ production (13), and expression of this receptor was completely eliminated after anti-MHC-I treatment (Supplemental Fig. 2D). We also examined the innate NK cell subset, hepatic ILC1 cells (14), which demonstrated enhanced proliferation and IFN-γ production after M1/42 treatment (Supplemental Fig. 2E, F).

The proliferation and activation seen post M1/42 treatment was not restricted to NK cells and MP T cells. Marked enhancement of Ki-67 expression was observed in $CD3^-CD11c^+$ dendritic cells (DC) and $CD3^-CD11b^+$ monocyte populations, but not by $CD3^-CD19^+$ B lymphocytes (Fig. 3A). One likely explanation for the induced proliferation of DC and

monocytes was the enhanced production of GM-CSF by activated NK cells and MP T cells following M1/42 treatment (Supplemental Fig. 3A) accompanied by enhanced expression of the macrophage colony stimulating factor 1 receptor (CSF1R) (Supplemental Fig. 3B). The enhanced proliferation of DC and monocytes, was accompanied by elevated expression of MHC-I and MHC-II which was also seen on B lymphocytes (Supplemental Fig. 3C–E). The enhanced expression of MHC antigens is likely due to the increased production of IFN-γ by activated NK cells (15). IL-15 transcription by DC and monocytes (Fig. 3B) was elevated as was IL-15Rα expression by all APC subsets (Fig. 3C). Enhanced expression of IL-15Rα on APC by M1/42 treatment required the presence of NK cells as well as IFN-γ (Fig. 3C). The *in vivo* expansion of MP $CD4^+$ and $CD8^+$ T cells following M1/42 administration was driven by the trans-presentation of IL-15, as it was completely abolished by treatment with anti-CD122 (16–18) (Fig. 3D). It is likely that the IFN-γ/IL-15 axis is responsible for the proliferation and expansion of both NK cells and MP T cells, respectively (19–21).

M1/42 was administered to mice that were concurrently infected with acute LCMV, Armstrong strain (22). On d 15 post-infection (post viral clearance), mice treated with M1/42 contained expanded numbers of viral antigen-specific $CD4^+$ and $CD8^+$ T cells which produced higher levels of IFN-γ (Supplemental Fig. 4 A, B). Simultaneous treatment with M1/42 and infection with chronic LCMV, clone 13, resulted in death of the majority of animals within a week post infection secondary to a cytokine storm. A similar outcome was observed when PD-L1 deficient mice were infected with clone 13 (22). To avoid the cytokine storm, we treated chronically infected mice every 3 d for 14 d beginning on d 20 after infection and analyzed the mice on d 37. This regimen resulted in an enhanced number of MP $CD4^+$ and $CD8^+$ viral antigen-specific T cells with marked enhancement of IFN-γ production (Fig. 4A, B). Most notably, M1/42-treated animals demonstrated almost complete clearance of virus from multiple infected non-lymphoid sites (Fig. 4C).

The augmentation of immune responses by M1/42 treatment was not restricted to anti-viral immunity but could also be extended to tumor immunity. M1/42 treatment markedly inhibited the growth of the MC38 colon adenocarcinoma and depletion of either NK cells or $CD8^+$ T cells completely reversed the anti-tumor effects of M1/42 (Fig. 4D), indicating the requirement of both innate and adaptive responses to generate tumor immunity. M1/42 treatment also markedly reduced the growth of the PD1-resistant melanoma (B16F10) (Fig. 4E, F and Supplemental Fig. 4C), and also enhanced the number of tumor-specific $CD8^+$ T cells and their capacity to produce IFN-γ and Granzyme B (Supplemental Fig. 4D). M1/42 was effective in suppression of the growth of B16F10 when given as late as 7 d after tumor implantation (Fig. 4G).

NK cells represent a rapidly responding population of cells that can manifest effector functions including cytolysis, the secretion of cytokines/chemokines, and augmentation of antibody dependent cellular cytotoxicity in an antigen-independent manner (1). This pro-inflammatory NK cell program is regulated by the interaction of inhibitory receptors with MHC-I (either murine Ly49 or human KIR). Recent studies have suggested that blockade of NKIR with mAbs by mimicking the effects of MHC-I downregulation represents a promising approach to the augmentation of the anti-tumor effects of NK cells (23). However, a single NKIR is only present on a subpopulation of NK cells and this may account for some

of the failures of anti-inhibitory receptor immunotherapy (24). Our studies demonstrate that profound activation of NK cell function can be induced by globally blocking Ly49/MHC-I interactions. IFN-γ production by unleashed NK cells functions in a forward feedback loop to enhance NK cell activation. The NK cell production of IFN-γ and other cytokines then activates APC with the subsequent production of IL-15 which in turn activates NK cells and drives MP $CD4^+$ and $CD8^+$ activation and expansion thereby augmenting the adaptive immune response.

All functions of M1/42 in wild type mice were also observed in mice that lack FcR (data not shown), so it is unlikely that the Fc domain of the antibody plays a major role. Furthermore, *in vitro*, mAb M1/42 directly inhibited the binding of soluble Ly49 antigens to their cognate MHC-I targets. These results differ from the recent observations of Bern et al (25) who demonstrated that disruption of MHC-I/NK inhibitory interactions by down regulation of MHC-I expression in adult mice by administration of tamoxifen to $B2m^{fl/fl}R26\text{-}Cre\text{-}ER^{T2}$ mice resulted in NK cell tolerance. Variation between these studies may be explained by differences in the kinetics and persistence of the effects of mAb administration and Cre-mediated deletion of MHC-I expression. The functional effects of KIR/MHC-I and Ly49/MHC-I interactions in the human and mouse are similar, but the structural bases differ. Human KIR bind MHC-I in a region at least partially competitive with the TCR site, while murine Ly49 do not compete (6, 26). Nevertheless, it may be possible to generate an anti-human MHC-I mAb that mimics the properties of M1/42. Taken together, our findings demonstrate that targeted blocking of KIR/MHC-I interactions represents a promising target for the potentiation of immune responses to tumors and pathogens, and may offer a new approach for improved vaccination strategies (27–30).

Supplementary Material

Refer to Web version on PubMed Central for supplementary material.

Acknowledgements

We thank M. Butcher, H. Yamane, N. Mansoori, K. Wang, N. Sherani and J. Jiang for supplying reagents and assistance with many experimental protocols. Tetramers were provided by the NIH Tetramer Core Facility.

This work was supported by the Division of Intramural Research, National Institute of Allergy and Infectious Diseases.

Abbreviations used in this article

β2m	β2-microglobulin
CM	central memory
CTV	cell trace violet
DC	dendritic cell
EM	effector memory
KIR	killer-immunoglobuiin-like receptor

LCMV	lymphocytic choriomeningitis virus
MP	memory phenotype

References

1. Vivier E, Raulet DH, Moretta A, Caligiuri MA, Zitvogel L, Lanier LL, Yokoyama WM, and Ugolini S 2011 Innate or adaptive immunity? The example of natural killer cells. Science 331: 44–49. [PubMed: 21212348]
2. Karlhofer FM, Ribaudo RK, and Yokoyama WM 1992 MHC class I alloantigen specificity of Ly-49+ IL-2-activated natural killer cells. Nature 358: 66–70. [PubMed: 1614533]
3. Karre K 1997 How to recognize a foreign submarine. Immunol. Rev. 155: 5–9. [PubMed: 9059878]
4. Karre K, Ljunggren HG, Piontek G, and Kiessling R 1986 Selective rejection of H-2-deficient lymphoma variants suggests alternative immune defence strategy. Nature 319: 675–678. [PubMed: 3951539]
5. Li Y, and Mariuzza RA 2014 Structural basis for recognition of cellular and viral ligands by NK cell receptors. Front. Immunol. 5: 123. [PubMed: 24723923]
6. Natarajan K, Dimasi N, Wang J, Mariuzza R, and Margulies D 2002 Structure and function of natural killer cell receptors: Multiple molecular solutions to self, nonself discrimination. Ann. Rev. Immunol 20: 853–885. [PubMed: 11861620]
7. Ozato K, Hansen TH, and Sachs DH 1980 Monoclonal antibodies to mouse MHC antigens. II. Antibodies to the H-2Ld antigen, the products of a third polymorphic locus of the mouse major histocompatibility complex. J. Immunol. 125: 2473–2477. [PubMed: 7191868]
8. Natarajan K, Boyd LF, Schuck P, Yokoyama WM, Eliat D, and Margulies DH 1999 Interaction of the NK cell inhibitory receptor Ly49A with H-2Dd: identification of a site distinct from the TCR site. Immunity 11: 591–601. [PubMed: 10591184]
9. Gangaplara A, Martens C, Dahlstrom E, Metidji A, Gokhale AS, Glass DD, Lopez-Ocasio M, Baur R, Kanakabandi K, Porcella SF, and Shevach EM 2018 Type I interferon signaling attenuates regulatory T cell function in viral infection and in the tumor microenvironment. PLoS pathogens 14: e1006985. [PubMed: 29672594]
10. Wang J, Whitman M, Natarajan K, Tormo J, Mariuzza R, and Margulies D 2002 Binding of the natural killer cell inhibitory receptor Ly49A to its major histocompatibility complex class I ligand - Crucial contacts include both H-2D(d) and beta(2)-microglobulin. J. Biol. Chem. 277: 1433–1442. [PubMed: 11696552]
11. Matsumoto N, Mitsuki M, Tajima K, Yokoyama WM, and Yamamoto K 2001 The functional binding site for the C-type lectin-like natural killer cell receptor Ly49A spans three domains of its major histocompatibility complex class I ligand. J. Exp. Med. 193: 147–158. [PubMed: 11148219]
12. Stallcup KC, Springer TA, and Mescher MF 1981 Characterization of an anti-H-2 monoclonal antibody and its use in large-scale antigen purification. J. Immunol. 127: 923–930. [PubMed: 6167633]
13. Robbins SH, Nguyen KB, Takahashi N, Mikayama T, Biron CA, and Brossay L 2002 Cutting edge: inhibitory functions of the killer cell lectin-like receptor G1 molecule during the activation of mouse NK cells. J. Immunol. 168: 2585–2589. [PubMed: 11884419]
14. Seillet C, Belz GT, and Huntington ND 2016 Development, Homeostasis, and Heterogeneity of NK Cells and ILC1. Curr. Top. Microbiol. Immunol. 395: 37–61. [PubMed: 26305047]
15. Goldszmid RS, Caspar P, Rivollier A, White S, Dzutsev A, Hieny S, Kelsall B, Trinchieri G, and Sher A 2012 NK cell-derived interferon-gamma orchestrates cellular dynamics and the differentiation of monocytes into dendritic cells at the site of infection. Immunity 36: 1047–1059. [PubMed: 22749354]
16. Richmond JM, Strassner JP, Zapata L Jr., Garg M, Riding RL, Refat MA, Fan X, Azzolino V, Tovar-Garza A, Tsurushita N, Pandya AG, Tso JY, and Harris JE 2018 Antibody blockade of IL-15 signaling has the potential to durably reverse vitiligo. Sci.Trans. Med. 10: eaam 7710.
17. Yokoyama S, Watanabe N, Sato N, Perera PY, Filkoski L, Tanaka T, Miyasaka M, Waldmann TA, Hiroi T, and Perera LP 2009 Antibody-mediated blockade of IL-15 reverses the autoimmune

intestinal damage in transgenic mice that overexpress IL-15 in enterocytes. Proc. Nat. Acad. Sci. USA 106: 15849–15854. [PubMed: 19805228]

18. Anton OM, Peterson ME, Hollander MJ, Dorward DW, Arora G, Traba J, Rajagopalan S, Snapp EL, Garcia KC, Waldmann TA, and Long EO 2019 Trans-endocytosis of intact IL-15Ralpha-IL-15 complex from presenting cells into NK cells favors signaling for proliferation. Proc. Nat. Acad. Sci. USA 117:522–531. [PubMed: 31871169]
19. Alter G, and Altfeld M 2011 Mutiny or scrutiny: NK cell modulation of DC function in HIV-1 infection. Trends in Immunol. 32: 219–224. [PubMed: 21411368]
20. Lusty E, Poznanski SM, Kwofie K, Mandur TS, Lee DA, Richards CD, and Ashkar AA 2017 IL-18/IL-15/IL-12 synergy induces elevated and prolonged IFN-gamma production by ex vivo expanded NK cells which is not due to enhanced STAT4 activation. Mol. Immunol. 88: 138–147. [PubMed: 28644973]
21. Santana Carrero RM, Beceren-Braun F, Rivas SC, Hegde SM, Gangadharan A, Plote D, Pham G, Anthony SM, and Schluns KS 2019 IL-15 is a component of the inflammatory milieu in the tumor microenvironment promoting antitumor responses. Proc. Nat. Acad. Sci. USA 116: 599–608. [PubMed: 30587590]
22. Barber DL, Wherry EJ, Masopust D, Zhu B, Allison JP, Sharpe AH, Freeman GJ, and Ahmed R 2006 Restoring function in exhausted CD8 T cells during chronic viral infection. Nature 439: 682–687. [PubMed: 16382236]
23. Andre P, Denis C, Soulas C, Bourbon-Caillet C, Lopez J, Arnoux T, Blery M, Bonnafous C, Gauthier L, Morel A, Rossi B, Remark R, Breso V, Bonnet E, Habif G, Guia S, Lalanne AI, Hoffmann C, Lantz O, Fayette J, Boyer-Chammard A, Zerbib R, Dodion P, Ghadially H, Jure-Kunkel M, Morel Y, Herbst R, Narni-Mancinelli E, Cohen RB, and Vivier E 2018 Anti-NKG2A mAb Is a Checkpoint Inhibitor that Promotes Anti-tumor Immunity by Unleashing Both T and NK Cells. Cell 175: 1731–1743. [PubMed: 30503213]
24. Carlsten M, Korde N, Kotecha R, Reger R, Bor S, Kazandjian D, Landgren O, and Childs RW 2016 Checkpoint Inhibition of KIR2D with the Monoclonal Antibody IPH2101 Induces Contraction and Hyporesponsiveness of NK Cells in Patients with Myeloma. Clin. Canc. Res. 22: 5211–5222.
25. Bern MD, Parikh BA, Yang L, Beckman DL, Poursine-Laurent J, and Yokoyama WM 2019 Inducible down-regulation of MHC class I results in natural killer cell tolerance. J. Exp. Med. 216: 99–116. [PubMed: 30559128]
26. Radaev S, and Sun PD 2003 Structure and function of natural killer cell surface receptors. Ann. Rev. Biophysics and Biomolecular Structure 32: 93–114.
27. Van Elssen CH, Oth T, Germeraad WT, Bos GM, and Vanderlocht J 2014 Natural killer cells: the secret weapon in dendritic cell vaccination strategies. Clin. Canc. Res. 20: 1095–1103.
28. Malmberg KJ, Sohlberg E, Goodridge JP, and Ljunggren HG 2017 Immune selection during tumor checkpoint inhibition therapy paves way for NK-cell “missing self” recognition. Immunogenetics 69: 547–556. [PubMed: 28699110]
29. van Montfoort N, Borst L, Korrer MJ, Sluijter M, Marijt KA, Santegoets SJ, van Ham VJ, Ehsan I, Charoentong P, Andre P, Wagtmann N, Welters MJP, Kim YJ, Piersma SJ, van der Burg SH, and van Hall T 2018 NKG2A Blockade Potentiates CD8 T Cell Immunity Induced by Cancer Vaccines. Cell 175: 1744–1755.e1715. [PubMed: 30503208]
30. Koch J, Steinle A, Watzl C, and Mandelboim O 2013 Activating natural cytotoxicity receptors of natural killer cells in cancer and infection. Trends in Immunol. 34: 182–191. [PubMed: 23414611]

Key Points

Blockade of Ly49/MHC-I interactions by anti-MHC-I results in activation of NK cells.

IFN-γ produced by activated NK cells stimulates APC to produce IL-15.

Activated NK and T cells markedly augment anti-viral and anti-tumor immunity.

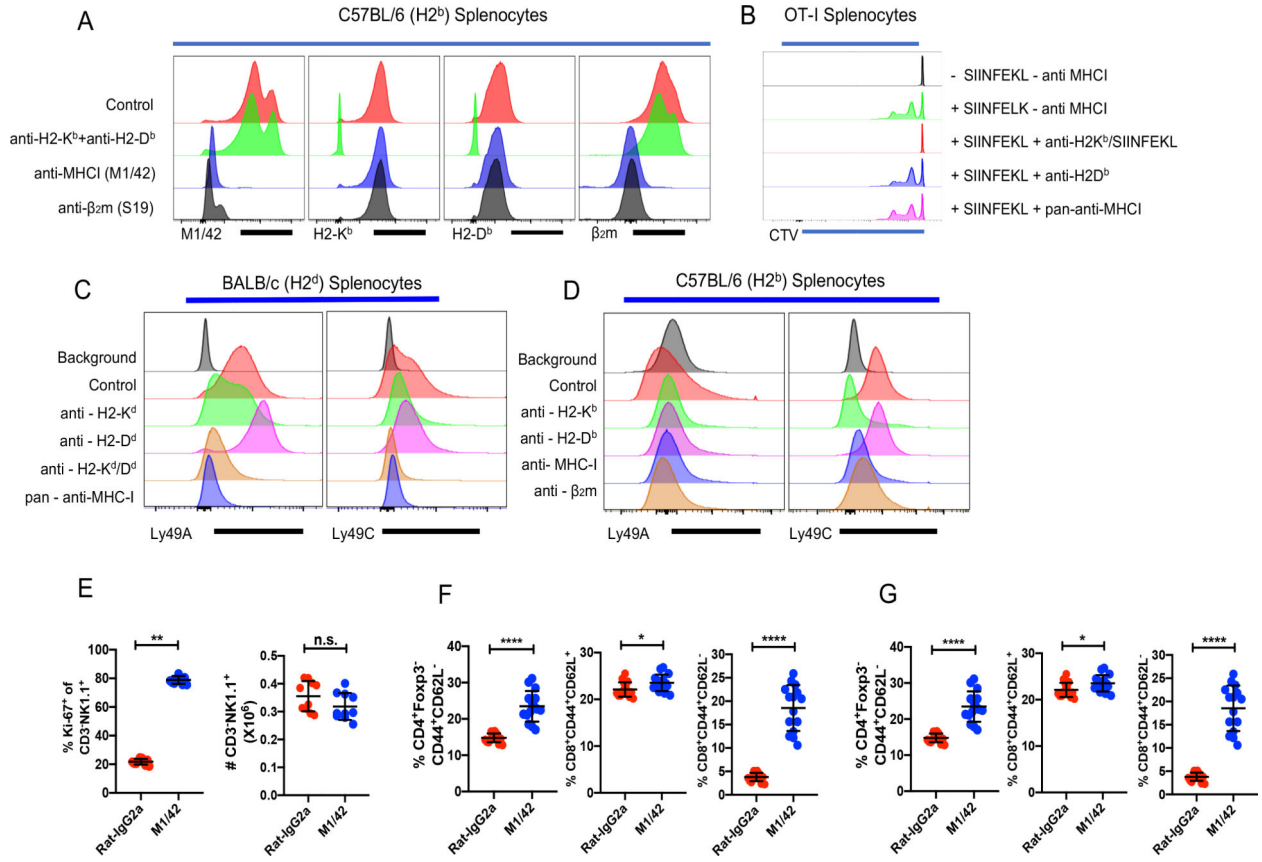

Figure 1.

M1/42 blocks the binding of anti-β_2m, blocks NK cell inhibitory receptor binding, and induces marked proliferation of NK and memory T cells. **(A)** Splenocytes from C57BL/6 ($H2^b$) mice were incubated with purified Rat-IgG2a, a mixture of anti-H2-K^b (AF6–88.5) and H2-D^b (28–14-8), pan-anti-MHC-I (M1/42) and β_2m (S19) antibody and then stained with different flourochrome tagged antibodies. (**B, C)** Splenocytes from BALB/c (H-2^d) and C57BL/6 (H-2^b), mice were incubated with biotinylated Ly49A or Ly49C recombinant proteins, blocked with the indicated mAb (unlabeled), anti-H2-K^b (SF1.1.10), anti-H2-K^d/D^d (34–1-2S), anti-H2-D^d (34–2-12), or anti-MHC-I (M1/42), and then stained with PE-Strepavidin. Panels A-C represent a representative experiment of four using 3 mice per group. (**D**) CTV-labeled splenocytes from OT-I mice were incubated with different anti-MHC-I antibodies (H2-K^b SIINFEKL (25-D1.16), H2-D^b (28–14-8), M1/42 and then cultured with $OVA_{257–264}$ for 48 h. $CD8^+$ T cell proliferation was measured by CTV dilution. This result is a representative experiment of two. (**E)** Rat-IgG2a or anti-M1/42 were injected (i.p.) every two d for six d. Ki-67 expression by and absolute number of $CD3^-NK1.1^+$ cells in spleen were determined on d 8. **(F)** Relative frequency, and absolute number of $CD4^+Foxp3^-$ EM T cells. (**G & H**) Relative frequency & absolute number of CM and EM $CD8^+$ T cells after isotype control or M1/42 treatment.

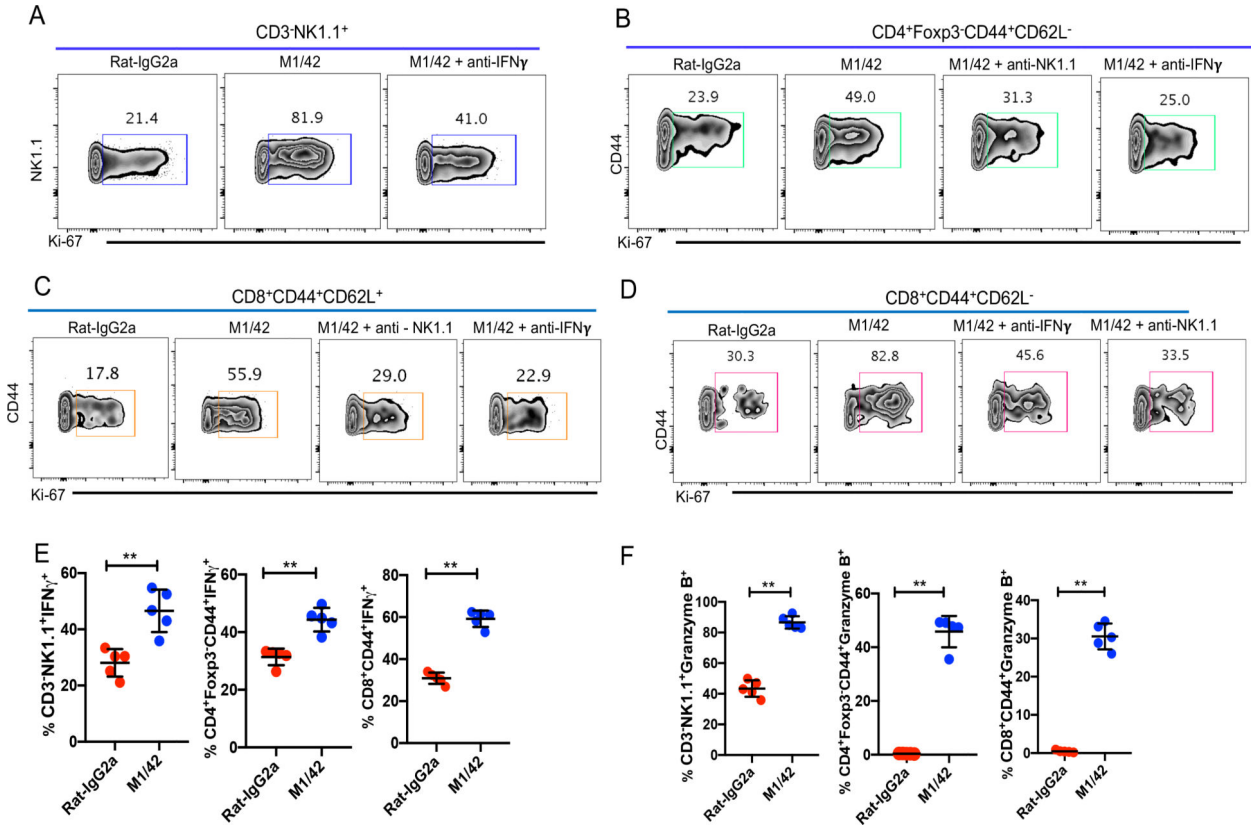

Figure 2.

M1/42 mediated enhancement of NK cell proliferation depends on IFN-γ, whereas MP T cell proliferation depends on both NK cells and IFNγ. **(A)** C57BL/6 mice were injected with M1/42 or control Rat-IgG2a, either alone or with a neutralizing anti-IFN-γ mAb every other d for 6 d. Ki-67 expression was analyzed after 8 d. (**B, C, D)** C57BL/6 mice were treated with M1/42 or the isotype control alone, or together with a depleting anti-NK1.1 or anti-IFNγ mAb for six d. Splenocytes were harvested on d 8 and Ki-67 expression of $CD4^+$ EM, $CD8^+$ CM and $CD8^+$ EM were determined. Panels A-D represent the result of one independent experiment of 3 using 5 mice per group. (**E, F, G)** Splenocytes from M1/42 or isotype control treated mice were harvested on d 8, incubated with PMA and ionomycin plus protein transport inhibitor cocktail for 4 h to measure production of IFN-γ and Granzyme B by NK cells and MP $CD4^+$ and $CD8^+$ cells.

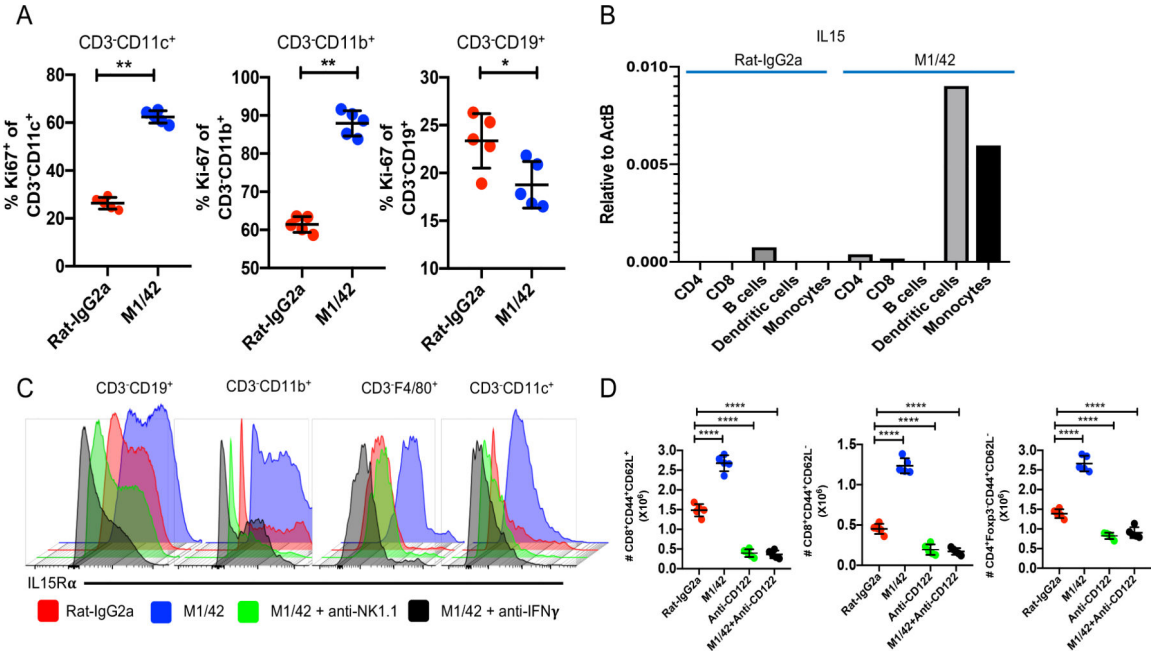

Figure 3.

M1/42 expands APC and activates IL-15 trans-presentation. **(A)** Ki67 expression of DC ($CD3^{-}CD11c^{+}$), monocytes ($CD3^{-}CD11b^{+}$), and B cells ($CD3^{-}CD19^{+}$) on d 8 after M1/42 treatment. (**B)** IL-15 transcription was measured by TaqMan™ real-time PCR from FACS sorted immune cells on d 8. The data are from one representative experiment of two. **(C)** IL-15Rα expression on splenic derived APC populations on d 8 after treatment with M1/42 or isotype control or M1/42 together with anti-NK1.1, or M1/42 together with anti-IFN-γ. The data are from one representative experiment of 3 performed using 3 mice per group. (**D**) Total numbers of $CD8^{+}$ CM or EM and $CD4^{+}$ EM T cells were determind after staining with M1/42, anti-CD122, or M1/42 together with anti-CD122.

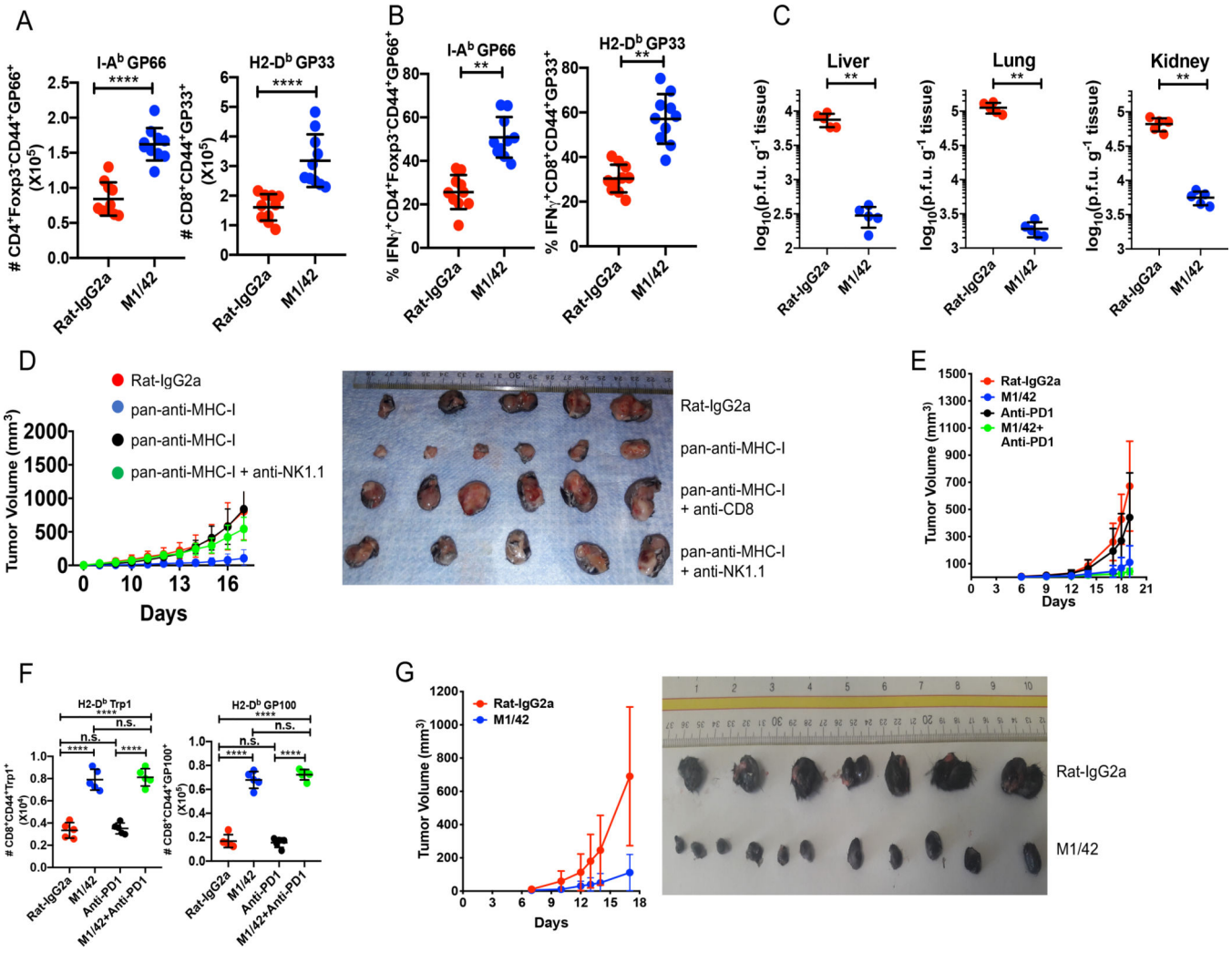

Figure 4.

M1/42 augments anti-viral and anti-tumor immunity. Chronic LCMV (clone 13) infected C57BL/6 mice were treated with M1/42 every 3 d from d 20 to d 33 and spleen cells were harvested on d 37 post-infection. Results are from one representative experiment of 3 using 10 mice per group. **(A)** Total number of tetramer positive $CD4^+$ and $CD8^+$ T cells in the spleen. **(B)** Percentage of IFN-γ-producing tetramer-positive $CD4^+$ and $CD8^+$ T cells. **(C)** Viral titers in the indicated tissues. **(D)** MC38 (0.2×10^6) colon adenocarcinoma cells were injected subcutaneously and mice were treated with M1/42 alone or together with anti-CD8 or anti-NK1.1 at 3 d intervals. Results are from one representative experiment of 2 using10 mice per group. Graphic representation of tumor volume, measured every 2–3 d (left panel). Tumor sizes from each group after 18 d of antibody treatment (right panel). **(E)** B16F10 tumor cells (1.25×10^5) were injected s.c, and mice were treated with M1/42 or isotype control alone, anti-PD-1 alone or the combination of M1/42 and anti-PD-1 every three d from d 3 to d 18. Results are from one representative experiment of two times using 10 mice per group. Tumor volumes were measured and plotted. **(F)** Total number of tumor-specific $CD8^+CD44^+GP100^+$ and $CD8^+CD44^+Trp1^+$ cells from tumor draining lymph nodes were

determined after 18 d. **(G)** B16F10 tumor cells were implanted s.c and mice were treated with anti-MHC-I every 3 d from d 7–18. Results are from one representative experiment of two using 10 mice per group. Tumor volumes were plotted (left panel) and relative tumor sizes were compared on d 18.